Ecological Applications, 30(8), 2020, e2188
© 2020 by the Ecological Society of America

Forest restoration treatments in a ponderosa pine forest enhance physiological activity and growth under climatic stress

ALAN J. TEPLEY,[1,2,4] SHARON M. HOOD,[3] CHRISTOPHER R. KEYES,[2] AND ANNA SALA[1,2]

[1]*Division of Biological Sciences, University of Montana, Missoula, Montana 59812 USA*
[2]*W.A. Franke College of Forestry & Conservation, University of Montana, Missoula, Montana 59812 USA*
[3]*Fire, Fuel and Smoke Science Program, Rocky Mountain Research Station, USDA Forest Service, Missoula, Montana 59808 USA*

Citation: Tepley, A. J., S. M. Hood, C. R. Keyes, and A. Sala. 2020. Forest restoration treatments in a ponderosa pine forest enhance physiological activity and growth under climatic stress. Ecological Applications 30(8):e02188. 10.1002/eap.2188

Abstract. As the climate warms, drought will increasingly occur under elevated temperatures, placing forest ecosystems at growing risk of extensive dieback and mortality. In some cases, increases in tree density following early 20th-century fire suppression may exacerbate this risk. Treatments designed to restore historical stand structure and enhance resistance to high-severity fire might also alleviate drought stress by reducing competition, but the duration of these effects and the underlying mechanisms remain poorly understood. To elucidate these mechanisms, we evaluate tree growth, mortality, and tree-ring stable-carbon isotope responses to stand-density reduction treatments with and without prescribed fire in a ponderosa pine forest of western Montana. Moderate and heavier cutting experiments (basal area reductions of 35% and 56%, respectively) were initiated in 1992, followed by prescribed burning in a subset of the thinned units. All treatments led to a growth release that persisted to the time of resampling. The treatments had little effect on climate–growth relationships, but they markedly altered seasonal carbon isotope signals and their relationship to climate. In burned and unburned treatments, carbon isotope discrimination ($\Delta^{13}C$) increased in the earlywood (EW) and decreased in the latewood (LW) relative to the control. The sensitivity of LW $\Delta^{13}C$ to late-summer climate also increased in all treatments, but not in the control. Such increased sensitivity indicates that the reduction in competition enabled trees to continue to fix carbon for new stem growth, even when the climate became sufficiently stressful to stop new assimilation in slower-growing trees in untreated units. These findings would have been masked had we not separated EW and LW. The importance of faster growth and enhanced carbon assimilation under late-summer climatic stress became evident in the second decade post-treatment, when mountain pine beetle activity increased locally, and tree mortality rates in the controls of both experiments increased to more than twice those in their respective treatments. These findings highlight that, when thinning is used to restore historical forest structure or increase resistance to high-severity fire, there will likely be additional benefits of enhanced growth and physiological activity under climatic stress, and the effects may persist for more than two decades.

Key words: carbon isotope discrimination; dendroecology; drought; forest restoration; ponderosa pine; prescribed fire; thinning; tree mortality.

INTRODUCTION

Incidents of extensive drought-driven forest dieback and tree mortality are becoming increasingly common in many regions globally, a trend likely to accelerate as rising temperatures drive increases in evaporative demand (Adams et al. 2009, Anderegg et al. 2013, Breshears et al. 2013, Allen et al. 2015). Drought affects forests both directly, by altering tree phenology and physiology (Bréda et al. 2006), and indirectly, by contributing to increases in the frequency, extent, or severity of disturbances by fire (e.g., by lengthening fire seasons and drying fuels; Abatzoglou and Williams 2016, Westerling 2016) or biotic agents (e.g., by enhancing bark beetle population growth while weakening tree defenses; Weed et al. 2013). In some cases, the impacts of drought or drought-related disturbances have been less severe in stands with lower tree density (Ruiz-Benito et al. 2013, Young et al. 2017, Restaino et al. 2019), leading to the premise that silvicultural thinning can ameliorate tree- and stand-level vulnerability to drought (Sohn et al. 2016, Bradford and Bell 2017).

Reducing stand density is also consistent with the restoration of historical forest structure in some landscapes, including dry ponderosa pine (*Pinus ponderosa*) forests of western North America, where frequent fires historically maintained stands at lower densities than

Manuscript received 20 September 2019; revised 28 January 2020; accepted 30 March 2020. Corresponding Editor: Emil Cienciala.

[4]E-mail: alan.tepley@umontana.edu

currently found (Allen et al. 2002). Fuel reduction treatments, involving thinning with or without prescribed fire, are widespread in ponderosa pine forests (Kalies and Yocom Kent 2016), including approximately 5,400 km^2 of United States federal land between 1999 and 2012 (Barnett et al. 2016). The primary objective of these treatments is typically to increase resistance to high-severity fire by reducing fuel loading (Fulé et al. 2012). The degree to which they also reduce vulnerability to drought and how long this effect persists remain poorly understood due to limited insight into the mechanisms by which competition alters tree responses to drought.

The influences of stand density on tree- and forest-level vulnerability to drought are commonly evaluated by comparing growth or mortality between thinned and unthinned stands. For instance, reductions in radial growth during the recent drought in northern California were less severe (i.e., trees showed higher resistance to drought; Lloret et al. 2011) in thinned than unthinned stands (Vernon et al. 2018). In other regions, growth increases at the end of a drought were larger or the return to pre-drought growth (recovery and resilience metrics of Lloret et al. 2011) occurred sooner in thinned than unthinned stands (D’Amato et al. 2013, Sohn et al. 2016, Bottero et al. 2017). Statistical models based on interactions between basal area and climate proxies better predicted tree mortality than models using either predictor alone, highlighting that responses to drought depend on stand density (Bradford and Bell 2017, Young et al. 2017).

Although studies quantifying the interacting influences of drought and stand density on tree growth and mortality provide insight into the effects of specific drought events, they do not identify the mechanisms behind those responses, as needed to anticipate and predict future responses. The underlying mechanisms are better understood by analyzing growth and mortality responses along with direct measurements of changes in site characteristics (e.g., soil-water and nutrient relationships) and tree physiology following thinning treatments (Sala et al. 2005, Simonin et al. 2006). However, the labor required for such measurements typically limits their collection to a couple of years at a given site. Continuous measurements at the same site over multiple years to decades are extremely rare. Yet, such longer-term data may be essential for capturing gradual tree responses and the range of climatic conditions needed to more fully understand the effects of treatments.

Stable isotopes in tree rings are another source for insight into long-term variability in tree physiological responses to drought (Gessler et al. 2018) and alterations of those responses following stand-density manipulation (Sohn et al. 2014, 2016). Carbon isotope discrimination ($\Delta^{13}\text{C}$), for instance, provides a time-integrated approximation of the ratio of leaf internal to external CO_2 concentration during carbon assimilation, which is strongly affected by the processes influencing photosynthesis and stomatal conductance, including drought stress.

Retrospective assessments of the effects of stand density changes on tree-ring $\Delta^{13}\text{C}$ are usually based on values for whole tree-ring samples (McDowell et al. 2006, Sohn et al. 2016). However, $\Delta^{13}\text{C}$ signals can vary widely within each year of growth (Warren et al. 2001, Szejner et al. 2018), as is the case across much of western North America, where drought stress is typically lowest in spring to early summer, when earlywood (EW) is produced, but evaporative demand and soil-water deficits both increase later in the summer when latewood (LW) is produced. Because the majority of growth occurs in the spring to early summer, EW is likely to dominate the $\Delta^{13}\text{C}$ signal of whole tree rings, masking the LW signal, which may be more useful in interpreting how changes in stand density alter tree responses to drought (Voelker et al. 2019). Evaluating LW alone, however, could overlook important mechanisms by which trees ameliorate or are impaired by drought, such as shifts in the allocation of recently assimilated vs. older carbon stores for stem growth (Vaganov et al. 2009, Castagneri et al. 2018, Szejner et al. 2018). Long-term records of both EW and LW $\Delta^{13}\text{C}$ are needed to better understand how changes in stand density alter tree responses to drought.

Here, we seek to elucidate the mechanisms by which increased stand density and competition in the absence of frequent fire have altered tree vulnerability to drought by evaluating tree growth, mortality, and tree-ring $\Delta^{13}\text{C}$ responses to management treatments, including thinning with and without prescribed burning, in a ponderosa pine forest of western Montana. Our analyses span the 23-yr windows before and after treatments, enabling us to compare initial responses and the persistence of those changes under a range of variation in climate and external disturbance pressures (e.g., bark beetle activity). We seek to answer (1) how did the treatments alter trajectories of tree growth and $\Delta^{13}\text{C}$? (2) In what ways did the treatments alter the growth and $\Delta^{13}\text{C}$ responses to climate, and do those changes differ between EW and LW? (3) To what degree are these alterations of growth, $\Delta^{13}\text{C}$, and the relationships of both variables to climate reflected in different tree mortality rates between treated and untreated stands, and specifically, have the treatments reduced mortality rates compared to unthinned units?

Methods

Study area and experimental design

The Lick Creek Demonstration-Research Forest is a ponderosa pine-dominated forest (*Pinus ponderosa* var. *ponderosa* Douglas ex P. Lawson & C. Lawson) in the Bitterroot National Forest of western Montana (46.083° N, 114.245° W; Fig. 1). It spans elevations from 1,280 to 1,550 m along a south-facing slope. Annual precipitation (1981–2010) averages 378 mm (Abatzoglou et al. 2018), and the soil is strongly acidic sandy loam (DeLuca and Zouhar 2000). The forest was initially harvested between 1906 and 1911, with subsequent cuttings in the 1950s and 1960s to remove most trees that were retained during the initial harvest. Additional treatments include stand improvement cuttings and a thinning in part of the study area in 1967 (Smith and Arno 1999).

We evaluate the responses to the most recent thinning and prescribed burning treatments, which were implemented in two separate experiments: moderate and heavy thinning. We use the term “thinning” to indicate a density-reduction treatment. However, from a silvicultural perspective, the moderate thinning was a “commercial thinning,” and the heavy thinning was a “shelterwood treatment” that included an objective of promoting new regeneration (Smith and Arno 1999).

The moderate thinning experiment was conducted on 28 ha along the upper slope (Fig. 1). The objective was to reduce basal area by 40–50% and maximize the growth of the remaining stand. The heavy thinning experiment was conducted on 34 ha along the lower slope. The goals were to reduce basal area by two-thirds, while opening the canopy sufficiently to promote a second age class of ponderosa pine (Smith and Arno 1999). Both experiments favored retaining ponderosa pine and reducing the density of Douglas-fir (*Pseudotsuga menziesii* var. glauca (Mayr) Franco).

Each experiment includes a total of 12 management units (1.0–6.6 ha each), where three were left as untreated controls, and nine were thinned in the spring of 1992 (Fig. 1). Three of the treated units had no subsequent burning (hereafter, thin-only treatments). The other six were subjected to one of two prescribed burning treatments. In the moderate thinning experiment, three of the thinned units were burned in the fall of 1993 and three were burned in the spring of 1994 (hereafter, fall and spring burn treatments, respectively). In the heavy thinning, all burning was conducted in the spring of 1993, with three units burned when the duff was moist in early May and three burned under drier conditions later in the month (hereafter, wet and dry burn treatments, respectively; Smith and Arno 1999).

Twelve circular plots (0.0405 ha each; radius 11.35 m) were established within each experimental unit (144 plots per experiment, 288 total). All treated units were sampled in 1991 and 1993, before and after the thinning, respectively. Treated and control units were sampled again after the prescribed burning (1993 and 1994 in the heavy and moderate thinning experiments, respectively). All plots were resampled in 2005 and 2015. Initial responses were reported in Smith and Arno (1999), physiological responses in years 8 and 9 were reported by Sala et al. (2005), and 23-yr biomass and stand dynamics were reported in Clyatt et al. (2017) and Bowen (2017).

Tree-ring data

In summer 2016, we randomly selected 8 of the 12 plots within each unit and cored the nearest large

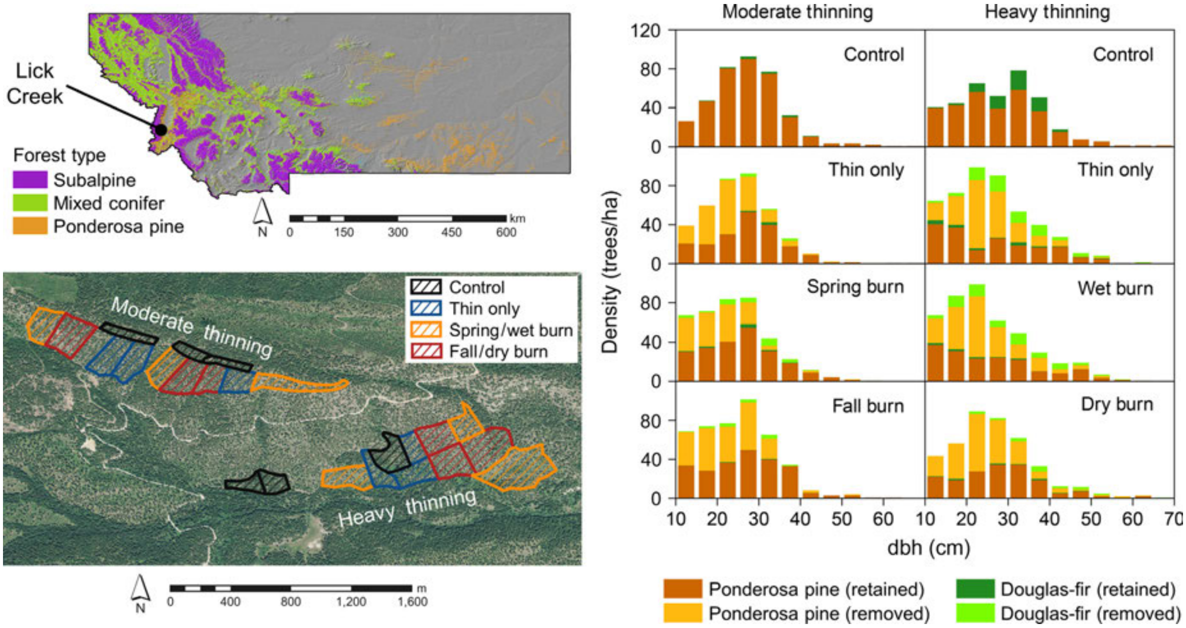

Fig. 1. The Lick Creek Demonstration-Research Forest of the Bitterroot National Forest in western Montana, USA (forest types are LANDFIRE biophysical settings; https://www.landfire.gov/bps.php). The aerial photo is NAIP imagery taken in 2009 (https://datagateway.nrcs.usda.gov/GDGHome_DirectDownLoad.aspx). The midslope area between the moderate and heavy thinning has also been thinned. A denser forest canopy characteristic of unmanaged conditions is visible along the lower edge of the photo. The stacked bar graphs at right were developed by comparing data collected before (1991) and just after completion of the treatments (1993 and 1994).

(>25.4 cm dbh) and small (≤25.4 cm dbh) ponderosa pine tree to the plot center, thereby sampling 16 trees per unit and 192 trees per experiment. We collected two cores per tree, on opposite sides of the tree at a mean height of 51 cm, with all cores 5.15 mm in diameter.

The first core per tree was used to calculate growth metrics: basal area increment (BAI), earlywood area increment (EWAI), latewood area increment (LWAI), and the proportion of latewood (PLW, where PLW = LWAI/BAI). We used the second core to calculate BAI before selecting a subset of these cores for stable-carbon isotope analyses. We scanned the cores at 1,200–2,400 dpi and measured ring width (all cores) and EW and LW width (the first core per tree) to the nearest 0.001 mm using CDendro Version 9.2 (Cybis Elektronik and Data AB 2018*a*). Crossdating was validated using COFECHA (Holmes 1983).

To calculate BAI, EWAI, and LWAI, we first estimated the distance to the pith from the first ring in each core using CooRecorder Version 9.2 (Cybis Elektronik and Data AB 2018*b*). We then summed this distance plus the radial increment for each ring to produce the bole radius (inside bark) at the end of each year of growth (r_t). Then we calculated BAI as $\pi(r_t^2 - r_{t-1}^2)$. We followed the same procedure to calculate EWAI and LWAI, with the exception that the outer radius for EWAI was the sum of all preceding ring widths plus the current EW. This value was then used as the inner radius for calculating LWAI. We averaged BAI across the two cores per tree to evaluate trends in BAI over time. For PLW, we used BAI values from only the core on which EW and LW were measured.

Stable-carbon isotope data

Trees from only the heavy thinning experiment were used for stable-carbon isotope analyses. Six cored trees per unit were selected at random from the total sampled, providing 18 trees per treatment (72 total). We excluded trees that established after 1930 to minimize the "juvenile effect" (McCarroll and Loader 2004, Leavitt 2010).

We used a scalpel to section each ring from 1969 to 2015 into EW and LW samples and pooled the samples from the six trees per unit (Leavitt 2008), providing one EW and one LW carbon isotope chronology for each unit, and three EW and LW chronologies per treatment. The chronologies include the treatment year (1992) plus each year over the 23-yr windows before and after treatments (1969–1991 and 1993–2015). We used a Wiley Mill (Thomas Scientific, Swedesboro, New Jersey, USA) to grind the samples to fine shavings, and we extracted the waxes, resins, and oils following Leavitt and Danzer (1993). Then, we homogenized the samples to a fine powder before sending them to the Stable Isotope Laboratory at Washington State University (Pullman, Washington, USA).

Stable-carbon isotope composition (the ratio of ^{13}C to ^{12}C) relative to the known Vienna Pee Dee Belemnite (VPDB) standard is expressed as δ^{13}C (μmol/mol) = ($R_{\text{sample}}/R_{\text{standard}} - 1$) × 1,000 and is driven primarily by the ratio of leaf internal to external CO$_2$ concentration (c_i to c_a), which reflects differences in the rates of photosynthesis and stomatal conductance. Because plant δ^{13}C depends on the δ^{13}C of the air source, we calculated carbon isotope discrimination (Δ^{13}C) as ($\delta^{13}C_{\text{air}} - \delta^{13}C_{\text{plant}}$)/($1 - \delta^{13}C_{\text{plant}}/1{,}000$) to remove trends in ambient δ^{13}C due to rising atmospheric CO$_2$ concentration (McCarroll and Loader 2004). For $\delta^{13}C_{\text{air}}$, we used the values provided in McCarroll and Loader (2004) and supplemented more recent values with the annual mean of the monthly values recorded at Mauna Loa, Hawaii (*available online*).[5]

Analyses

Growth responses and climate–growth relationships.—We compared growth responses among treatments over the post-treatment interval (1993–2015) by first conducting one mixed-design ANOVA (Khuri et al. 2011) for each experiment (moderate and heavy thinning) to determine whether the mean BAI differed among treatments, and whether those differences varied over time. We constructed the model using R package rstatix (Kassambara 2019), with BAI as the dependent variable, individual trees as the subjects, treatment as the between-subjects factor, and year as the within-subjects factor. If the mean BAI values differed significantly ($P < 0.05$) among treatments and those differences varied over time, we used Tukey's HSD test (R package multcomp; Hothorn et al. 2008) to determine which treatments differed significantly from each other in each year.

To evaluate climate–growth relationships, we standardized each growth metric (BAI, EWAI, and LWAI) to emphasize year-to-year variation while reducing the post-treatment growth release. For standardization, we first applied an adaptive power transformation to stabilize the variance of each series over time (Cook and Peters 1997). Then we used "Friedman's super smoother" to minimize the post-treatment growth release (Friedman 1984). We developed one chronology for each growth metric for each treatment, with all standardization conducted using ARSTAN Version 44h3 (Cook and Krusic 2014).

We used the residual chronologies (Cook and Peters 1997) to relate year-to-year variation in growth to five climate variables. The climate variables include monthly precipitation, maximum temperature (Tmax), vapor pressure deficit (VPD), and climatic water deficit, acquired at 4-km resolution from TerraClimate (Abatzoglou et al. 2018 ;data *available online*).[6] We also used the Palmer Drought Severity Index (PDSI) for western Montana (Montana's Division 1 of the National

---

[5] https://scrippsco2.ucsd.edu/data/atmospheric_co2/mlo.html

[6] http://www.climatologylab.org/terraclimate.html

Oceanic and Atmospheric Administration's divisional climate data; *available online*).[7]

We evaluated climate–growth relationships for each growth metric using bootRes (Zang and Biondi 2013) in R Version 3.5.0 (R Core Team 2018). Specifically, we calculated correlation functions with bootstrapped confidence intervals for the relationships between each growth metric and the five climate variables over each month from the previous April through the current September (Biondi and Waikul 2004). We compared climate–growth relationships over the 23-yr post-treatment portion of each chronology (1993–2015) to those over an equivalent section of each chronology before the treatments (1969–1991).

Treatment effects on $\Delta^{13}C$ and climate–$\Delta^{13}C$ relationships.—To evaluate how the treatments altered *intra*-annual variation in $\Delta^{13}C$, we first produced one EW and one LW $\Delta^{13}C$ chronology for each treatment of the heavy thinning experiment by averaging across the three replicates (i.e., units) within each treatment. We then calculated the *intra*-annual range of $\Delta^{13}C$ as the absolute value of the difference between the EW and LW $\Delta^{13}C$ for each year. To determine whether treatments altered these values, we used one-way ANOVA with treatment as a factor, constructing separate models for the pre- and post-treatment periods. We used Tukey's HSD test (R package multcomp; Hothorn et al. 2008) to identify which treatments differed significantly ($P < 0.05$) from each other during each time period.

We also identified the climatic conditions that most strongly influence EW and LW $\Delta^{13}C$ by evaluating the relationships between EW and LW $\Delta^{13}C$ and monthly climate variables. Following our approach for evaluating climate–growth relationships, we constructed correlation functions with bootstrapped confidence intervals (Zang and Biondi 2013) for the relationship between EW and LW $\Delta^{13}C$ chronologies and five climate variables over each month from the previous April through the current September. We conducted the analysis by treatment, analyzing pre- and post-treatment intervals separately.

We further evaluated how the treatments altered climate–$\Delta^{13}C$ relationships by first using the correlation functions in the post-treatment period to identify the 2–3 month window of strongest correlation between each climate variable and EW or LW $\Delta^{13}C$. Then we modeled the relationships between $\Delta^{13}C$ and each climate variable over those 2–3 month windows, while testing for differences between the pre- and post-treatment period. To do this, for each treatment and climate variable, we modeled $\Delta^{13}C$ as a function of climate plus time period (pre- vs. post-treatment) plus the interaction between climate and time period. Then, because we have three EW and three LW replicates for each treatment (i.e., one chronology per treated unit), we also allowed the slope and intercept of the relationship between $\Delta^{13}C$ and the climate variable to differ among the three replicates. For each treatment, we modeled the relationship between $\Delta^{13}C$ and each climate variable separately for EW and LW: 4 treatments × 5 climate variables = 20 models for EW and 20 for LW.

If the slope of the relationship between $\Delta^{13}C$ and the climate variable did not differ significantly among replicates ($P > 0.05$) before or after treatments, we averaged the $\Delta^{13}C$ values across the three replicates and constructed a simpler model of the mean $\Delta^{13}C$ as a function of climate, time period, and the interaction between climate and time period. Then, we calculated the coefficient of partial determination (partial R^2) to assess the additional variance in $\Delta^{13}C$ explained by the interaction term that allows the slope of the relationship between $\Delta^{13}C$ and climate to differ between pre- and post-treatment periods, compared to a reduced model where the slope does not differ by time period (Kutner et al. 2005).

Mortality rates.—To address whether the treatments reduced tree mortality, we calculated annual tree mortality rates in the permanent plots over each census interval. Post-treatment censuses were conducted in 1993 and 1994 in the heavy and moderate thinning experiments, respectively, and in 2005 and 2015 in both experiments. We limited the mortality analysis to ponderosa pine to enable comparisons to the tree-ring analyses. We also excluded trees that were <15 cm dbh in the first of each pair of censuses.

We composited mortality data across plots and units within each treatment, providing one mortality rate per census interval for each treatment. For each census interval, we calculated the annual mortality rate (m) following Sheil et al. (1995):

$$m = \left[1 - \left(\frac{N_t}{N_0}\right)^{1/t}\right] \times 100$$

where N_0 is the number of living trees present in the first of the two censuses, N_t is the number of those trees that survived to the next census, and t is the interval (in years) between censuses. Trees that were <15 cm dbh at the time of the first census but grew above the 15-cm dbh threshold before the second census were only included in our calculations of mortality rates over the second census interval.

Sample size for the moderate thinning was 1,276 and 1,321 trees for the 1994–2005 and 2005–2015 census intervals, respectively. In the heavy thinning experiment, trees in control units were not tagged until after the 1993 census, and only living trees were sampled during this census. Because we could not be certain which trees were alive in 1993 and died by 2005, we calculated mortality rates for only the treated units (n = 495 trees) over the 1993–2005 census interval. However, we calculated mortality rates for each treatment and the control over the 2005–2015 interval (n = 810 trees).

---

[7] https://www7.ncdc.noaa.gov/CDO/CDODivisionalSelect.jsp#

To assess whether the treatments reduced mortality rates compared to untreated controls, we calculated 95% confidence intervals using either the normal approximation to the binomial variance if more than five trees died over the census interval, or binomial probabilities if five or fewer trees died (Condit et al. 1995). Because we were interested in whether the treatments reduced mortality rates compared to untreated controls, we generated confidence intervals for a one-sided test. We applied a Bonferroni correction for the total number of comparisons ($n = 3$); for each experiment and census interval, we compared three treatments to one control, but we did not compare all pairs of treatments to each other.

We evaluated mortality rates in relation to one of the main drivers of ponderosa pine mortality, the mountain pine beetle (*Dendroctonus ponderosae* Hopkins), using Aerial Detection Survey (ADS) data of the US Forest Service (data for 1992–1999 were acquired directly from the USDA Forest Service, Northern Region, Forest Health Protection; data for 2000–2015 were acquired *online*).[8] We developed a proxy for local mountain pine beetle activity for each experiment by calculating the proportion of the area within a 500-m radius surrounding the experimental units in which mountain pine beetle impacts were recorded during each year from the year of thinning (1992) through 2015.

RESULTS

Stand-density reduction and growth responses

Reductions in tree density and basal area were similar across the different treatments within each experiment (Table 1). Averaged across treatments, the moderate thinning reduced stem density by 40% to 220 trees/ha and basal area by 35% to 13.7 m^2/ha. The heavy thinning reduced stem density by 60% and basal area by 56% to 181 trees/ha and 11.9 m^2/ha, respectively. In the moderate thinning, ponderosa pine comprised 91–96% of the pre-treatment stem density and 89–95% of the basal area, and it increased to 98% of both variables after treatments. Other tree species (primarily Douglas-fir) were better represented in the heavy thinning experiment. There, ponderosa pine averaged 87% of the pre-treatment trees and 82% of the basal area, and it increased to 95% of both variables following treatments (Table 1).

The reduction in competition led to a marked growth release that persisted over the 23 yr of our growth-response analysis (Fig. 2). Mean BAI values differed significantly ($P < 0.05$), both among treatments and over time within each experiment. In the moderate thinning experiment, the mean annual BAI of all treatments was significantly greater than the control ($P < 0.05$) by the year 2000, and it remained greater than the control but not significantly different among treatments through 2015 (Fig. 2a). Portions of the control and fall burn treatments were also thinned in 1967 (Smith and Arno 1999), which led to an increase in BAI in 1968. Higher growth rates persisted for about two decades before they converged to values similar to the other treatments for 3–5 yr before the 1992 thinning (Fig. 2a).

Growth responses were more variable among treatments of the heavy thinning (Fig. 2b). The thin-only treatment had the most abrupt growth release, with BAI significantly greater than the control each year from

TABLE 1. Comparison of stand conditions before and immediately following treatments (data are for all live trees >10 cm dbh; species other than ponderosa pine include Douglas-fir, lodgepole pine, Engelmann spruce, grand fir, subalpine fir, and quaking aspen).

	Pre-treatment (1991)				Post-treatment (1993–1994)			
	All species		Ponderosa pine		All species		Ponderosa pine	
Treatment	Density (trees/ha)	Basal area (m^2/ha)	Density (%)	Basal area (%)	Density (trees/ha)	Basal area (m^2/ha)	Density (%)	Basal area (%)
Moderate thinning								
Control					378	24.0	97.5	96.9
Thin only	356	21.0	96.3	95.1	199 (44)	13.2 (37)	97.9	97.4
Spring burn	352	19.3	91.2	89.2	230 (35)	13.4 (31)	96.7	96.6
Fall burn	400	22.9	95.7	95.1	232 (42)	14.6 (36)	99.4	99.4
Treatment mean†	370	21.1	94.4	93.1	220 (40)	13.7 (35)	98.0	97.8
Heavy thinning								
Control					369	26.1	83.1	81.7
Thin only	470	29.0	82.0	77.2	198 (58)	12.7 (56)	91.7	91.7
Wet burn	474	26.2	85.2	81.6	172 (64)	10.9 (58)	96.0	97.6
Dry burn	401	25.6	93.0	88.1	172 (57)	12.1 (53)	96.0	95.3
Treatment mean†	448	26.9	86.7	82.3	181 (60)	11.9 (56)	94.6	94.9

Note: Values in parentheses represent the percent reduction in stem density and basal area relative to the pre-treatment value.
†Treatment mean represents the mean across all treated units, excluding the control.

---

[8] https://www.fs.usda.gov/main/r1/forest-grasslandhealth/

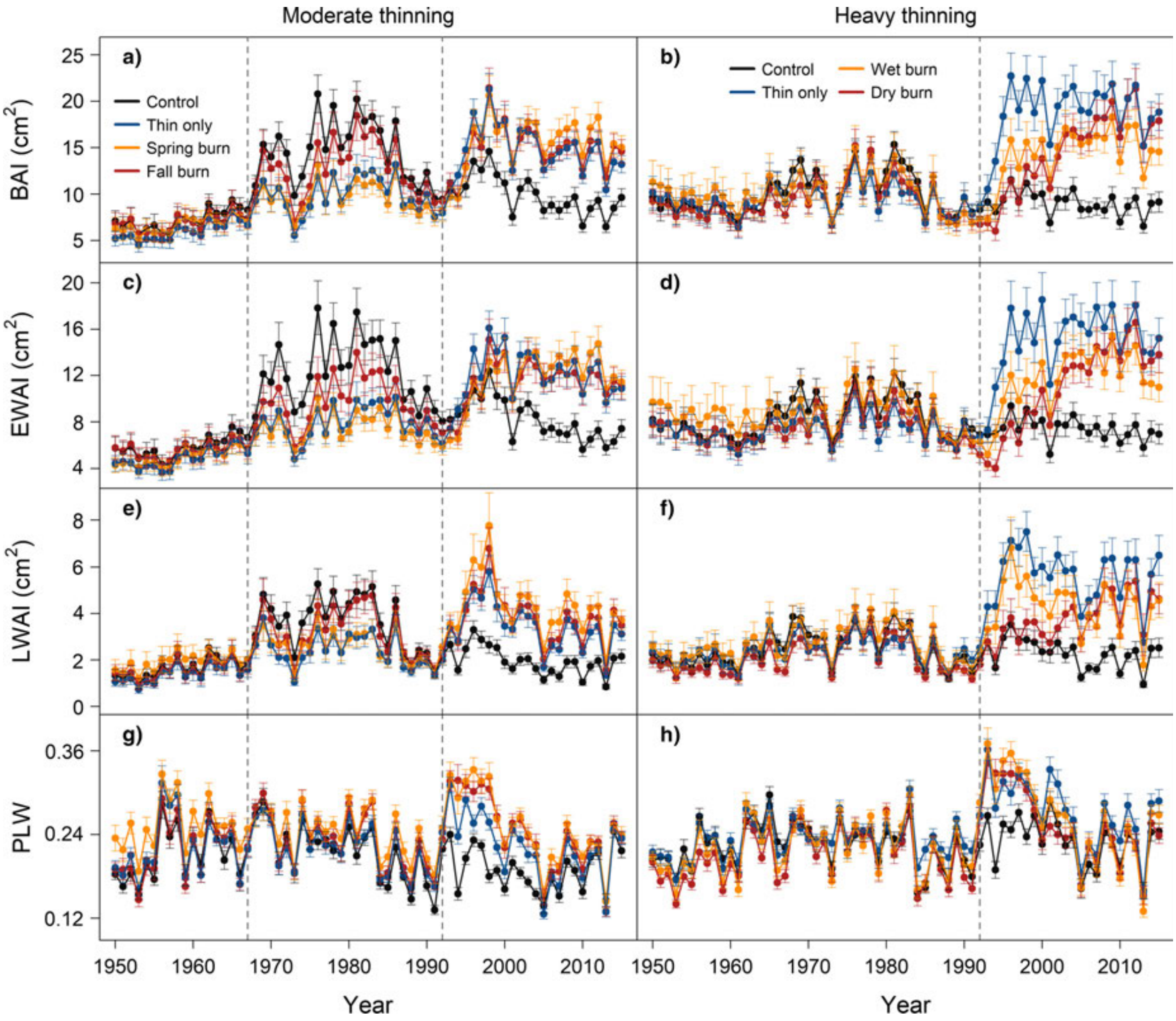

FIG. 2. Growth responses to the 1992 thinning followed by prescribed burning in 1993 and 1994, including basal area increment (BAI; a and b), earlywood area increment (EWAI; c and d), latewood area increment (LWAI; e and f), and the proportion of latewood (PLW; g and h). Values are means ± SE. Dashed vertical lines represent the year of thinning (1992) plus the year of an earlier thinning treatment (1967) conducted in portions of the current moderate thinning experiment. See Appendix S1: Fig. S1 for curves of each growth metric after standardization to minimize the post-treatment growth release.

1994 to 2015 ($P < 0.05$). The response was more gradual in the two thin and burn treatments, where BAI was not significantly greater than the control until 2003. The more gradual growth response was probably due to fire-caused injuries. For instance, crown scorch was recorded on 50% of trees in the wet burn and 62% in the dry burn during the first post-treatment plot census (summer 1993). Despite differences in the initial growth response, the mean annual BAI of all treatments remained significantly greater than the control but not different among treatments from 2003 through 2015 (Fig. 2b).

EWAI, LWAI, and PLW responses generally followed those of BAI, with two key exceptions (Fig. 2). First, PLW of all treatments in both experiments increased abruptly relative to the controls and the pre-treatment values (mean of 0.23; Fig. 2g, h). This increase was apparent by 1993 and lasted until 2004. Thereafter, PLW of all treatments returned to values similar to the controls, even though all other growth metrics remained higher than the controls (Fig. 2). Second, the wet burn treatment of the heavy thinning showed an abrupt initial increase in LWAI, resembling that in the thin-only treatment, even though its BAI and EWAI increased more gradually, similar to the dry burn (Fig. 2f).

Climate–growth relationships

For simplicity, we show climate–growth relationships for only the post-treatment period in the heavy thinning experiment (Fig. 3). Pre- and post-treatment results for

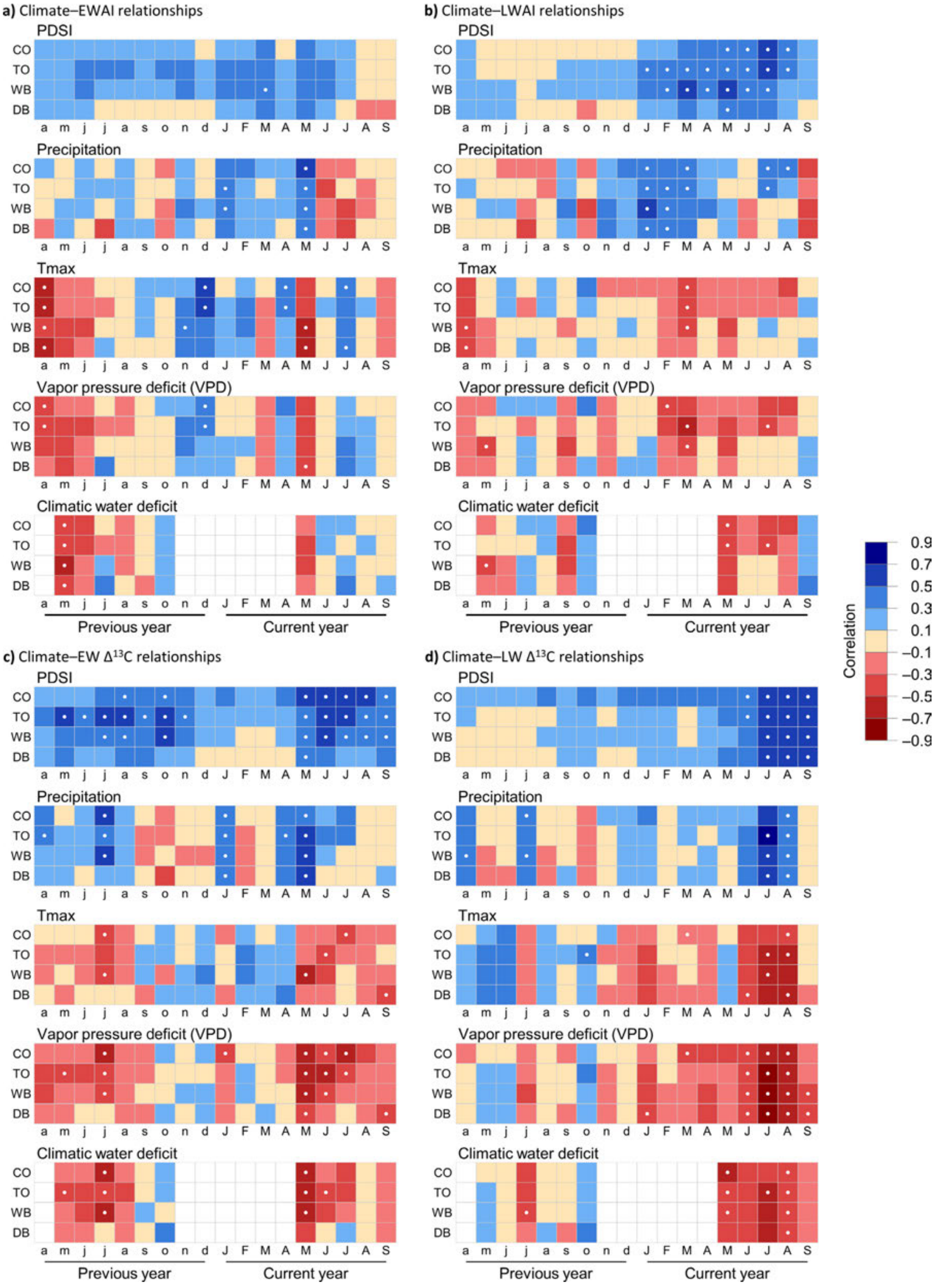

FIG. 3. Comparison of relationships of (a, b) earlywood (EW) and latewood (LW) growth and (c, d) EW and LW $\Delta^{13}C$ to monthly values of five climate variables: Palmer Drought Severity Index (PDSI), precipitation, maximum temperature (Tmax), vapor pressure deficit (VPD), and climatic water deficit. Relationships are shown for the post-treatment period (1993–2015) of the

heavy thinning experiment (CO, control; TO, thin only; WB, wet burn; DB, dry burn). Colors represent Pearson correlation coefficients, and white dots represent statistically significant correlations ($P < 0.05$), as determined from bootstrapped confidence intervals for the relationship to each climate variable for each month from April of the previous year through September of the current year (months are represented by lowercase letters for the previous year and capital letters for the current year). Correlations for growth metrics (EWAI and LWAI) range from –0.60 to 0.55, and correlations for $\Delta^{13}C$ range from −0.77 to 0.70. Climate–growth relationships for all growth metrics (BAI, EWAI, and LWAI) of both experiments are compared between pre- and post-treatment periods in Appendix S1, and we compare the pre- and post-treatment relationships between $\Delta^{13}C$ and climate for the heavy thinning experiment in Appendix S2. We use the same color scale in all figures relating growth or $\Delta^{13}C$ to climate to facilitate comparison of the strength of the relationships.

---

both experiments are compared in Appendix S1. After standardizing chronologies to focus on year-to-year variation, the post-treatment climate–growth relationships differed little among treatments (Fig. 3a, b; Appendix S1: Figs. S2–S5), except for a reduction in the sensitivity of LW growth to late-summer climate in the two thin and burn treatments of the heavy thinning (Fig. 3b).

Cool, moist conditions early in the growing season were favorable for EW growth, with all EWAI chronologies positively related to PDSI and precipitation and negatively related to Tmax, VPD, and climatic water deficit in the spring to early summer (Fig. 3a). All EWAI chronologies were also negatively related to Tmax, VPD, and climatic water deficit early (April through June) in the previous growing season (Fig. 3a). The months of strongest correlation between EW growth and climate and the strength of those correlations varied to some degree between pre- and post-treatment intervals. However, these differences were consistent across treated and control chronologies, suggesting they reflect the weather patterns of each time period rather than treatment effects (Appendix S1: Figs. S4, S5).

LW growth was related to both late-summer climate and precipitation during the preceding winter. Before treatments, all LWAI chronologies were positively related to late-summer PDSI and precipitation and negatively related to late-summer Tmax, VPD, and climatic water deficit (Appendix S1: Figs. S4, S5). These relationships persisted following treatments for all chronologies of the moderate thinning, but only for the control and thin-only treatments of the heavy thinning (Fig. 3b). The two thin and burn treatments of the heavy thinning showed reduced sensitivity to July and August climate. The climate–growth relationships also suggest that winter snowpack contributes to a soil-water reservoir important for LW growth. Correlations between LWAI and winter precipitation were strongly positive for treated and control chronologies of both experiments before and after treatments (Fig. 3b; Appendix S1: Figs. S4, S5).

Treatment effects on $\Delta^{13}C$

Treatment effects on $\Delta^{13}C$ were evaluated for only the heavy thinning experiment. The most distinct change following treatments was an amplification of the *intra*-annual variation, driven by increases in EW $\Delta^{13}C$ and decreases in LW $\Delta^{13}C$ in each treatment relative to the control (Fig. 4a–d). Before treatments, each year's EW $\Delta^{13}C$ exceeded that of the LW by an average ranging from 1.18‰ in the wet burn to 1.37‰ in the control and thin-only treatments, with no statistically significant differences ($P > 0.05$) among treatments (Fig. 4e). Following treatments, however, the *intra*-annual range increased to 1.68‰, 1.69‰, and 1.76‰ in the dry burn, thin-only, and wet burn treatments, respectively, all of which were significantly greater ($P < 0.05$) than that of the control (1.12‰; Fig. 4f).

The decrease in LW $\Delta^{13}C$ relative to control was apparent by the second-year post-treatment and was similarly abrupt under all treatments (Fig. 4a–c). By contrast, the increase in EW $\Delta^{13}C$ relative to the control occurred sooner in the thin-only treatment than in either of the two thin and burn treatments (Fig. 4a–c).

Treatment effects on climate–$\Delta^{13}C$ relationships

For EW and LW, $\Delta^{13}C$ was most strongly related to climate early and late in the growing season, respectively, suggesting that xylem was composed largely of carbon fixed close to the time of stem growth (Fig. 3c, d; climate–$\Delta^{13}C$ relationships for the pre-treatment period are shown in Appendix S2). During the post-treatment period, EW $\Delta^{13}C$ tended to increase under cool, moist conditions early in the growing season. It was positively correlated with precipitation in the spring (April and May) and PDSI from May through the end of the growing season (Fig. 3c). EW $\Delta^{13}C$ was also negatively related to VPD and climatic water deficit in May and June. In addition, there was a tendency for higher EW $\Delta^{13}C$ in response to cool, moist conditions in the previous growing season (Fig. 3c). Lagged relationships were weaker, however, for all treatments and the control over the pre-treatment period (Appendix S2: Fig. S1), suggesting the differences reflect the weather patterns of the two time periods rather than treatment effects.

Following treatments, LW $\Delta^{13}C$ of treated and control chronologies tended to increase under cool, moist conditions and decrease under warm, dry conditions late in the growing season (Fig. 3d). Correlations were positive and statistically significant ($P < 0.05$) for precipitation in July and August and PDSI in July through September. Correlations between LW $\Delta^{13}C$ and Tmax, VPD, and climatic water deficit were strongly negative in July and August and statistically significant for nearly all chronologies (Fig. 3d). There were few instances of statistically significant correlation between LW $\Delta^{13}C$ and

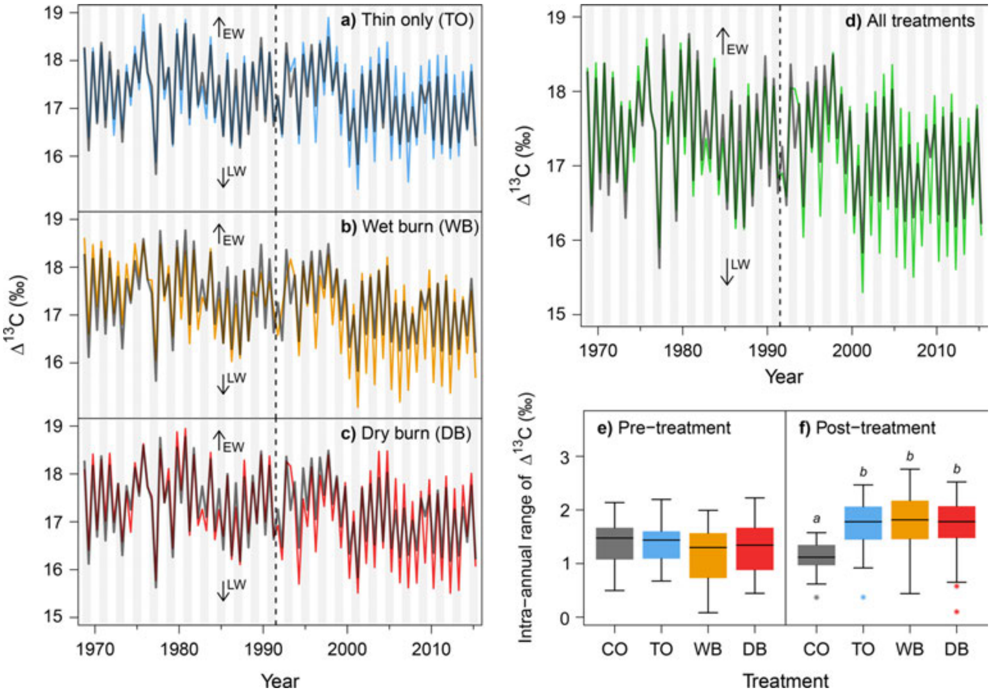

FIG. 4. Comparison of Δ^{13}C chronologies (means of the three units within each treatment) among treatments and controls of the heavy thinning experiment. Peaks and troughs are EW and LW, respectively. Colored and gray curves in panels a–c represent treated and control (CO) chronologies, respectively. In panel d, the mean of all treated chronologies (green) is compared to the control (gray). Alternating vertical gray and white shading in panels a–d represents odd- and even-numbered years, respectively. The *intra*-annual range of variation in Δ^{13}C is compared among chronologies for the pre- and post-treatment intervals in panels e and f, respectively, with different letters representing statistically significant differences ($P < 0.05$). Box plot midlines show medians, box edges show the interquartile range (IQR), and whiskers extend to the most extreme data point that is no more than 1.5 times the IQR beyond the upper or lower quartile.

climate prior to the current June or July. However, for several consecutive months beginning in winter to early spring, the control maintained stronger positive correlations with PDSI and negative correlations with VPD than the treated chronologies (Fig. 3d). Though not statistically significant, the stronger correlations to climate in the months preceding LW growth in control chronologies suggests the treatments may have reduced the dependence on carbon fixed earlier in the year for LW growth.

Although EW Δ^{13}C increased in all treated chronologies relative to the control (Fig. 4), the relationships between EW Δ^{13}C and climate differed little between pre- and post-treatment periods, except for a slight weakening of the relationship under several treatment–climate variable models (Fig. 5a). Responses were similar across replicates of each treatment for EW and LW models. Thus, we show only the average response per treatment in Fig. 5 (see Appendix S3 for regression coefficients for EW and LW models). For the control, the slope of the relationship between EW Δ^{13}C and climate after treatments did not differ from that over the pre-treatment period ($P > 0.05$). The interaction term that allowed the slope of the relationship to differ by time period explained essentially no additional variance in Δ^{13}C compared to a simpler model without the interaction (partial $R^2 \leq 0.02$ for all climate variables). After treatments in the dry burn, by contrast, EW Δ^{13}C became less responsive (i.e., the slope of the relationship became significantly gentler) to most climate variables in the spring to early summer ($P < 0.05$ and the partial R^2 ranged from 0.11 to 0.13 for PDSI, VPD, and climatic water deficit; $P \leq 0.10$ for Tmax). EW Δ^{13}C also became less responsive to PDSI after the thin-only treatment ($P < 0.05$, partial $R^2 = 0.12$; Fig. 5a).

The relationships of LW Δ^{13}C to late-summer climate consistently became stronger (i.e., the slope of the relationship became steeper) following all treatments, meaning that warm, dry conditions in late summer more strongly reduced LW Δ^{13}C after treatments than before (Fig. 5b). The relationship of LW Δ^{13}C to climate did not differ between pre- and post-treatment periods for any climate variable in the control ($P > 0.05$, partial $R^2 \leq 0.02$). However, a steepening of the relationship is apparent for each climate variable under all three treatments, with the change in slope statistically significant ($P < 0.05$) for precipitation, VPD, and climatic water deficit in nearly all treatments and for Tmax in the wet

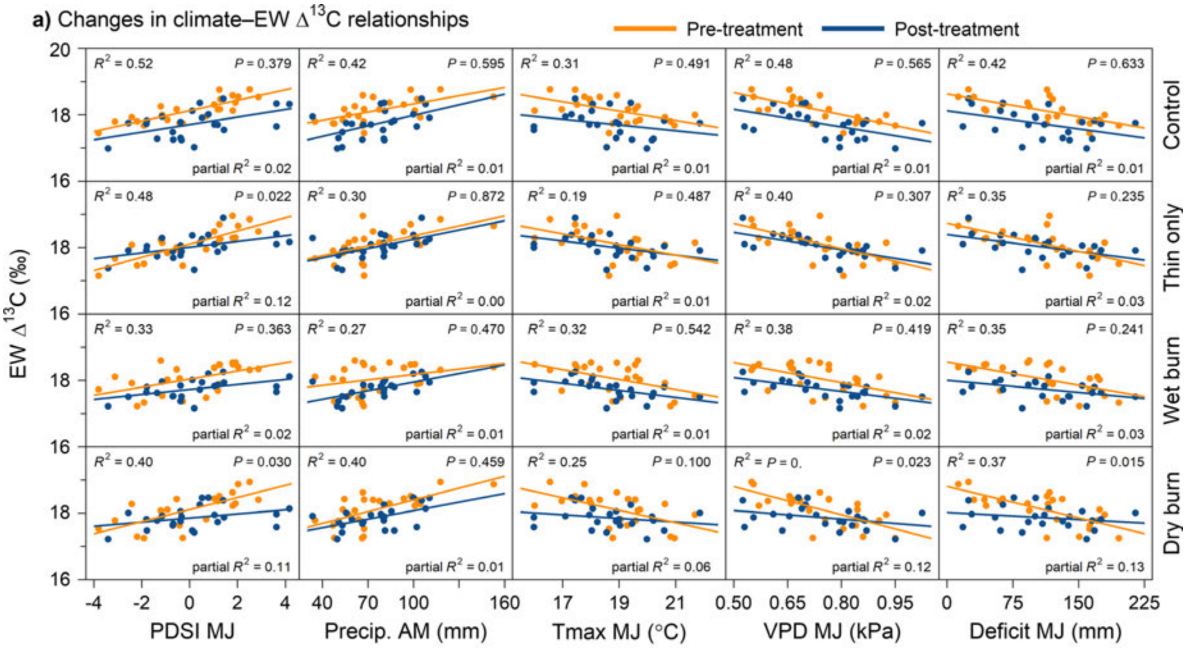

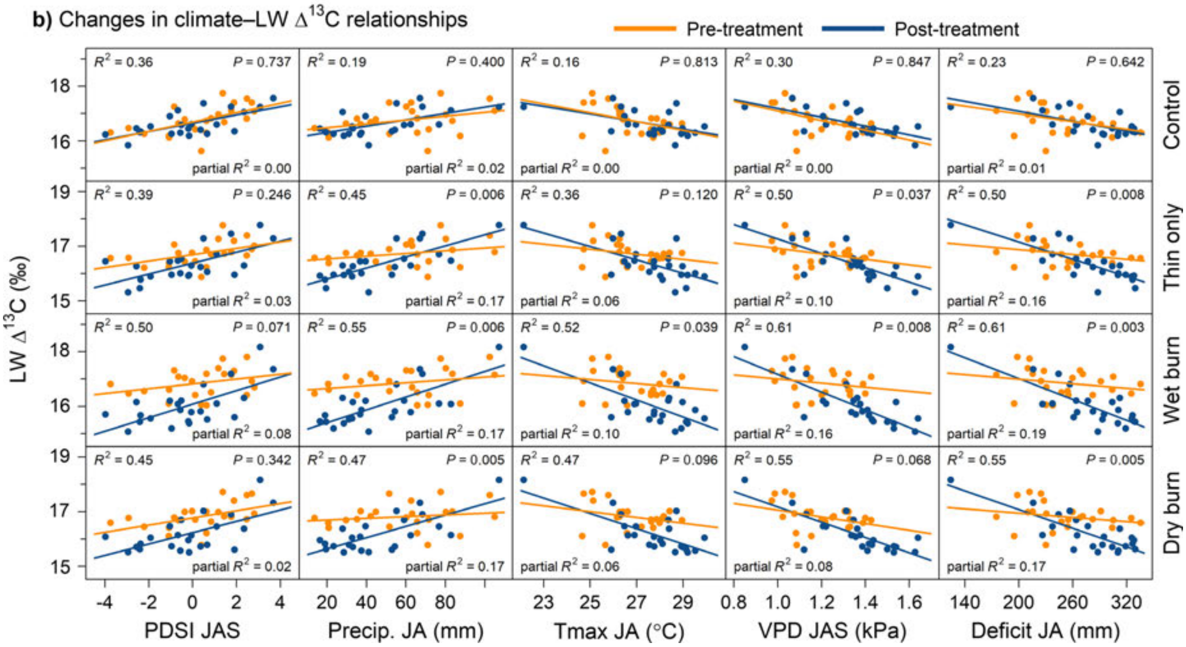

FIG. 5. Comparison of changes in the relationship between five climate variables and (a) EW Δ^{13}C and (b) LW Δ^{13}C. Panels are arranged with each row representing a different treatment and each column representing a different climate variable: Palmer Drought Severity Index (PDSI), precipitation (Precip.), maximum temperature (Tmax), vapor pressure deficit (VPD), and climatic water deficit (Deficit). The climate variables represent the average (or sum for precipitation) of the variable over the two- or three-month window in which it was most strongly related to Δ^{13}C based on Fig. 3 (MJ, May–June; AM, April–May; JAS, July–August–September; JA, July–August). The *P* values are for the interaction term that allows the slope of the relationship between Δ^{13}C and climate to differ between pre- and post-treatment periods. The partial R^2 represents the additional variance in Δ^{13}C explained by that interaction term, compared to a reduced model that does not allow the slope of the relationship to differ by time period.

burn. The interaction term that allowed the slope to differ by time period substantially increased the variance explained in LW Δ^{13}C for all climate variables (partial R^2 ranged from 0.06 to 0.19), with the exception of a weaker effect on the relationship to PDSI (partial R^2 ranged from 0.02 to 0.08; Fig. 5b).

Mortality rates

Tree mortality rates were similarly low (≤1% per yr) in treatments and controls over the first post-treatment census interval (1993 or 1994 through 2005; Fig. 6). They did not differ significantly from the control ($P > 0.05$) in any treatment of the moderate thinning (we could not calculate mortality rates for the control of the heavy thinning over this census interval because trees had not been tagged; see *Methods*). Mountain pine beetle activity increased over the next census interval (2005–2015), with aerial surveys documenting beetle impacts between 2011 and 2014, including more than 70% of the area within 500 m of both experiments in 2012 and 2014 (Fig. 6a). Over this interval, mortality rates increased to 1.98% per yr and 1.34% per yr in the controls of the moderate and heavy thinning, respectively. Both values were significantly greater ($P < 0.05$) than those found in their respective treatments, where the mortality rates (≤0.82% per yr and ≤0.42% per yr under the moderate and heavy thinning experiments, respectively) remained similar to those found under lower mountain pine beetle pressure during the previous census interval (Fig. 6).

Discussion

Forest restoration treatments in a second-growth ponderosa pine forest had substantial effects on tree growth and physiology that persisted for at least 23 yr. In response to our first question, the reduction of competition altered trajectories of tree growth and $\Delta^{13}C$ by contributing to a sustained growth release (Fig. 2) and amplifying the *intra*-annual variation in $\Delta^{13}C$ by increasing EW $\Delta^{13}C$ and decreasing LW $\Delta^{13}C$ relative to controls (Fig. 4). These responses were similar for all treatments other than a more gradual increase in growth and EW $\Delta^{13}C$ in burned than unburned treatments of the heavy thinning experiment.

For our second question regarding the effects of thinning on the growth and $\Delta^{13}C$ responses to climate, we found little difference in climate–growth relationships between treated and control chronologies other than a slight reduction in LW growth sensitivity to late-summer climate in the two thin and burn treatments of the heavy thinning (Fig. 3b). This difference likely had little influence on tree growth given that LW accounts for only a small portion of annual growth and the relationship of LW growth to winter precipitation remained strong in all treatments. The treatments had little effect on EW $\Delta^{13}C$ sensitivity to climate (Fig. 5a). However, we found a substantial increase in LW $\Delta^{13}C$ sensitivity that was similarly strong in burned and unburned treatments (Fig. 5b).

The implications of these changes for reducing tree vulnerability to drought and drought-related stresses (question 3) became evident over the second post-treatment plot census interval (2005–2015), when mountain pine beetle activity increased, and tree mortality rates in the controls of each experiment increased to more than twice that of their respective treatments (Fig. 6).

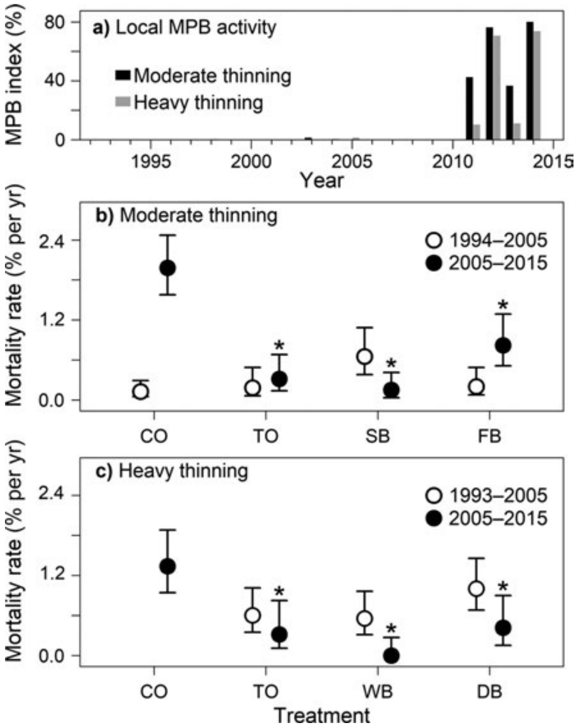

Fig. 6. Comparison of (a) trends in local mountain pine beetle (MPB) activity, and (b, c) tree mortality rates in the moderate and heavy thinning experiments, respectively. The MPB index represents the proportion of the area within a 500-m radius surrounding the experimental units in which MPB activity was recorded in ADS surveys. Mortality rates for the control of the heavy thinning experiment were not calculated because trees were not tagged until after the initial sampling. Error bars for mortality rates are Bonferroni-corrected confidence intervals for a one-sided test comparing each treatment to the respective control. Asterisks above the error bars for the treatment represent a significantly lower mortality rate ($P < 0.05$) than the control for the respective time period. Treatments are abbreviated as CO, control; TO, thin only; SB, spring burn; FB, fall burn; WB, wet burn; and DB, dry burn.

Importance of comparing $\Delta^{13}C$ in EW vs. LW

Our finding that after treatments EW and LW $\Delta^{13}C$ changed in opposite directions relative to the control (i.e., $\Delta^{13}C$ increased in the EW and decreased in the LW; Fig. 4) illustrates the importance of evaluating *intra*-annual variation in tree-ring stable-carbon isotope signals (Vaganov et al. 2009, Castagneri et al. 2018, Szejner et al. 2018). Previous findings regarding the effect of thinning on $\Delta^{13}C$ and the related intrinsic water-use efficiency (iWUE; the ratio of net photosynthetic assimilation, A, to stomatal conductance, g_s) vary, from findings that thinning increased iWUE (Navarro-Cerrillo et al. 2019), or it decreased iWUE due to greater increases in g_s than A (Giuggiola et al. 2016), to interpretations that iWUE was driven primarily by atmospheric CO_2 and climate but not competition (Fernández-de-Uña et al. 2016). Our findings suggest these discrepancies may be driven, in part, by analyzing whole tree rings rather than focusing on seasonal patterns. For instance, when we convert $\Delta^{13}C$ to iWUE (Farquhar et al. 1989), the seasonal oscillation persists (i.e., low iWUE in the EW and high iWUE in the LW, with an amplification of this pattern following treatments; Fig. 7a–d). However, if we estimate annual iWUE by averaging EW and LW values, weighted by the EWAI and LWAI for each year, the estimated whole-ring values mask the response to treatments, leaving the increase in iWUE in response to rising atmospheric CO_2 as the dominant trend in all chronologies (Fig. 7e).

Had we analyzed $\Delta^{13}C$ responses in whole tree rings, we would have found little effect of thinning, or we would have attempted to account for the few minor differences among treatments (e.g., small differences in iWUE between burned and unburned treatments from 1994 to 1998; Fig. 7e). However, our interpretations inevitably would have been inconsistent with the more detailed insight we gained by separating EW and LW.

Treatments enhanced C assimilation under late-summer climatic stress

Because EW comprises the majority of annual growth, the post-treatment increase in BAI under all treatments was driven primarily by an increase in EW growth (EWAI) relative to the controls (Fig. 2). LW forms under lower soil moisture and higher evaporative demand, but LW growth (LWAI) kept pace with the increase in EW under all treatments. In fact, the annual proportion of LW (PLW) increased for about a decade (Fig. 2). This ability of LW to keep up with the increase in EW growth has important implications for understanding how the treatments altered tree physiology and growth in the face of climatic stress.

The pattern of higher $\Delta^{13}C$ (lower iWUE) in EW than LW (Figs. 4, 7) is consistent with a strategy to maximize C assimilation at the expense of water loss when water is readily available early in the growing season. For all treatments, the post-treatment increase in EW growth relative to the controls (Fig. 2c, d) coincides with the increase in EW $\Delta^{13}C$ (decrease in EW iWUE; Figs. 4, 7), suggesting the EW growth release was driven in part by increases in stomatal conductance (g_s) and leaf-level photosynthetic rates (A), where the increase in g_s outweighed that in A. These interpretations are consistent with field measurements of A and g_s in 2001 and 2002 under the moderate thinning (Sala et al. 2005). The field data also show that foliage mass per tree increased following treatments, which further contributes to the increase in EW growth.

The post-treatment increase in foliage produced under favorable moisture conditions early in the growing

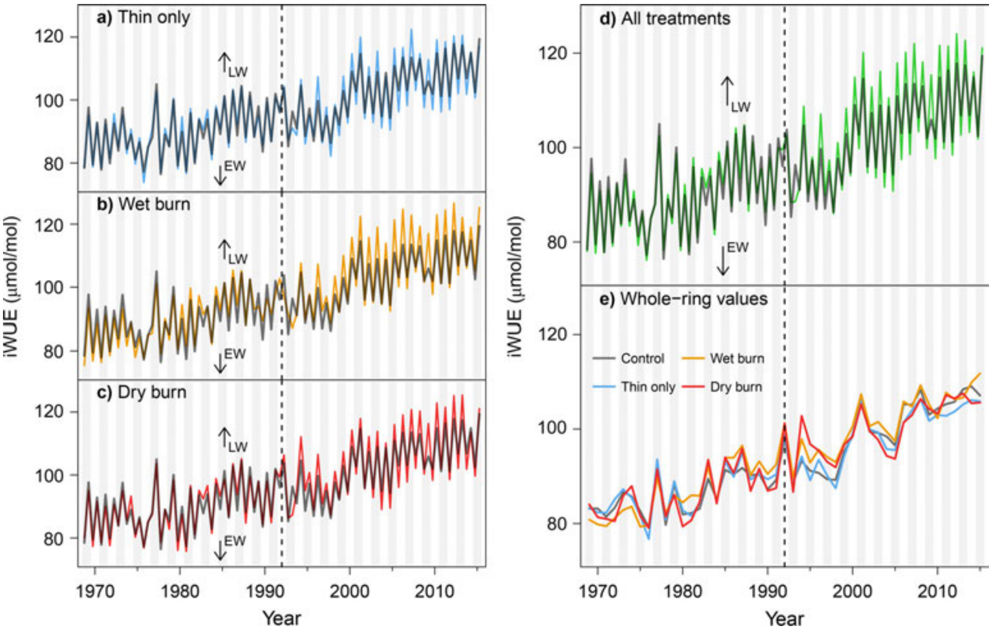

Fig. 7. Comparison of trends in intrinsic water-use efficiency (iWUE) among the mean chronologies for treated and untreated units (iWUE = $c_a(b - \Delta^{13}C)/[1.6(b - a)]$, where c_a is atmospheric CO_2 concentration, a = 4.4‰, and b = 27‰, as described under *Stable-carbon isotope data* in the *Methods*). Colored and gray curves in panels a–c represent treated and control chronologies, respectively. In panel d, the control and the mean of all treatments are shown in gray and green, respectively. Estimated iWUE for whole-ring samples are shown in panel e, where whole-ring values were calculated as EW iWUE$_t$ × (EWAI$_t$/BAI$_t$) + LW iWUE$_t$ × (LWAI$_t$/BAI$_t$). The subscript, t, indicates that all calculations were repeated for each year of growth. Alternating vertical gray and white shading represents odd- and even-numbered years.

season could leave trees more vulnerable to drought as they need to continue to supply water to larger crowns when evaporative demand increases and soil-water becomes more limiting in late summer (Jump et al. 2017). At first, this interpretation may seem to be supported by our findings that LW Δ^{13}C decreased (Fig. 4) and the relationship between LW Δ^{13}C and late-summer climate became steeper (i.e., a given level of climatic stress more strongly reduced LW Δ^{13}C) after all treatments but not in the control (Fig. 5b). However, this interpretation is not consistent with our finding of increased LW growth after treatments (Fig. 2e, f), nor with previous findings that trees in all treatments of the moderate thinning had higher July predawn water potential (suggesting lower whole tree water stress) than control trees, and they maintained higher A and g_s than the controls from late June through late August (Sala et al. 2005).

Rather than being indicative of increased foliage area leaving trees at greater risk of late-summer drought, we suggest that the reduction in LW Δ^{13}C and the strengthening of the relationship between LW Δ^{13}C and climate after treatments (Fig. 5b) indicates that trees in treated units were able to fix C and incorporate it into new stem growth under more severe climatic stress than trees in untreated units. For *Pinus* species, leaf gas exchange may be minimal in late summer because high evaporative demand and intense competition for limited water force stomatal closure (Martínez-Vilalta et al. 2004). The weaker relationship between LW Δ^{13}C and late-summer climate before treatments and for the controls in the post-treatment period suggests that in denser stands, it took less severe climatic stress to substantially reduce or prevent new assimilation (Vaganov et al. 2009, Castagneri et al. 2018).

Increases in the amount of, or access to, limited soil-water resources following thinning likely contribute to enhanced C assimilation under late-summer climatic stress in the treated units. At low elevations in western Montana, winter snowpack contributes to a deep soil-water reservoir important for late-summer tree growth (Martin et al. 2018), consistent with our finding that LW growth was positively correlated with winter precipitation (Fig. 3b). Although we have no data on how the treatments altered soil-water content deep in the profile, the ability of trees to maintain greater LW growth under all treatments than the controls (Fig. 2) supports that either soil-water content increased with fewer trees competing for the limited water supply, or that trees had greater access to soil-water due to expansion of their fine-root systems. Yet, despite differences in the amount of, or access to soil-water resources, the additional LW growth would have occurred under high evaporative demand, leading to low stomatal conductance, low Δ^{13}C, and high iWUE (Novick et al. 2016). With lower soil-water availability or more limited access to soil-water, trees in untreated units likely ceased new C assimilation at lower evaporative demand, leading to weaker relationships between LW Δ^{13}C and climate (Fig. 5b).

Thinning in a Southwestern (United States) ponderosa pine forest also led to higher predawn leaf water potential (Kolb et al. 1998) and faster growth (McDowell et al. 2006), and it increased the *inter*-annual variation in tree-ring carbon (Δ^{13}C) and oxygen (δ^{18}O) stable isotope signals (Sohn et al. 2014). Yet, in contrast to our study, where treatment effects on EW and LW Δ^{13}C persisted at least through the end of our 23-yr analysis (Fig. 4), the effects of thinning on whole-ring Δ^{13}C in the Southwest were limited primarily to years 5–12 following the initial thinning (McDowell et al. 2006). In that study, repeated thinning maintained stands at their post-treatment basal area, and the growth increase persisted at least through year 40, but tree-ring Δ^{13}C differed little between thinned and unthinned stands beyond the 12th year after the initial thinning. Our finding that treatment effects on Δ^{13}C persisted throughout the 23-yr post-treatment period might reflect the greater temporal resolution provided by evaluating EW and LW separately, where whole-ring values could mask important treatment effects (Fig. 7).

Thinning in Southwestern ponderosa pine stands also strengthened the correlation between tree-ring δ^{18}O and summer relative humidity (Sohn et al. 2014). Compared to trees in thinned stands, the weaker δ^{18}O sensitivity to summer climate and the muted *inter*-annual variation in stable isotope signals for slower-growing trees in unthinned stands were interpreted as driven by chronic water stress, where a limited ability to fix new C in late summer led to greater dependence on stored carbohydrates for stem growth. We found the muted stable isotope signals in control trees even more pronounced when focusing on *intra*-annual patterns (Figs. 4, 7), providing greater mechanistic insight into how stand density alters physiological activity under drought stress.

An intriguing finding is the short-term increase in the proportion of LW (PLW) observed from 1993 to about 2004 in all treated chronologies (Fig. 2). Expansion of crown area and fine-root systems in response to reduced competition could explain this result. Because carbon allocation to stem growth is generally a lower priority than allocation to new foliage or fine roots (Waring and Pitman 1985), we might expect a short-term, proportional reduction in allocation to stem growth while trees readjust to the additional above- and belowground resources made available following thinning. If this biomass calibration occurred primarily while water availability was relatively high early in the growing season but not under drier conditions in late summer, we would expect reduced allocation to EW growth, and a corresponding proportional increase in LW growth. Eventually, as new foliage and fine-root growth equilibrated to the post-treatment growing conditions, the sink strength for new foliage and roots would have decreased and proportional allocations to EW and LW growth would have returned to pre-treatment levels (Fig. 2g, h).

Interestingly, the time until PLW returned to pre-treatment levels roughly corresponds to the time it would have taken for a complete turnover of foliage (i.e., until all foliage produced before treatments was lost and replaced by foliage produced after the treatments).

Treatments enhanced resistance to a moderate increase in bark beetle pressure

The treatments enhanced resistance to at least one of the key drivers of ponderosa pine mortality (the mountain pine beetle), but the effects of treatments on tree mortality rates remained hidden for more than a decade until pressure (sensu Shore and Safranyik 1992) from this mortality driver increased. All treatments of the moderate and heavy thinning experiments maintained low tree mortality rates throughout the 23-yr post-treatment analysis period. However, when local mountain pine beetle activity increased during the second post-treatment plot census interval (2005–2015), mortality rates in the controls of both experiments increased to more than twice that of their respective treatments (Fig. 6). With mortality rates just under 2% per yr in the controls, the increase in mountain pine beetle activity (primarily in 2011–2014) was not a severe outbreak. Yet, the ability of treated units to maintain lower mortality rates during this period indicates the treatments enhanced tree resistance to this important driver of ponderosa pine mortality.

Increased resistance to bark beetle attack following thinning has been reported in ponderosa pine forests of other regions (Fettig et al. 2007, Zhang et al. 2013, Negrón et al. 2017), but additional work is needed to better understand the underlying mechanisms and how long the effects persist. Thin and burn treatments may increase tree defenses by increasing the number and sizes of resin ducts (Hood et al. 2016), and thereby increase resin flow (Kolb et al. 1998, McDowell et al. 2007). Greater tree-to-tree distances in thinned stands might also reduce the effectiveness of beetle dispersal and pheromone signaling, but relatively little is known about the degree of thinning needed to substantially alter these processes. Thinning might be less effective at increasing resistance to different bark beetle species in other forest types. For example, the probability of mortality during a spruce beetle outbreak in spruce–fir forests of the Colorado Front Range was influenced primarily by the size and age of individual host trees, whereas neighboring tree sizes and densities had only a minor influence (Bakaj et al. 2016).

Thin and burn treatments had little effect on growth and climate sensitivity beyond thinning alone

One of the few differences between burned and unburned treatments was a more gradual growth increase in the wet burn and dry burn treatments compared to the thin-only treatment of the heavy thinning (Fig. 2b). However, there was no corresponding difference between burned and unburned treatments of the moderate thinning (Fig. 2a). The sensitivity of LW growth to late-summer climate (precipitation, Tmax, and VPD) also decreased in the two thin and burn treatments, but not the thin-only treatment of the heavy thinning (Fig. 3b). This difference was largely due to differences in growth response over the first few years post-treatment, after which year-to-year variation in growth differed little among treatments (Appendix S1: Fig. S1).

The other main difference between burned and unburned treatments was a more gradual increase in EW $\Delta^{13}C$ in the two thin and burn treatments compared to the thin-only treatment of the heavy thinning (Fig. 4). This difference, along with the more gradual initial growth release in the thin and burn treatments, were both of short duration, and likely related to either fire-caused injuries (e.g., partial crown scorch) or alterations of soil nutrient cycling. Changes in inorganic nitrogen pools and nitrogen cycling rates were recorded in the first couple of years following burning in our study site (DeLuca and Zouhar 2000, Newland and DeLuca 2000), but the differences from unburned units were essentially lost by years 8–9 (Sala et al. 2005).

Conclusions

Our analyses support that the thinning and prescribed burning treatments commonly applied to restore historical stand structure and ecological processes in ponderosa pine forests or other forest types with a historical regime of frequent, low-severity fires are likely to enhance resistance to drought and biotic disturbances. Specifically, trees in thinned units were able to maintain physiological activity under greater climatic stress relative to trees in unthinned control units. We did not find that prescribed burning strengthened resistance to drought or bark beetles, at least under the intensity observed over the 23 yr since treatment in our study area. However, because the burning killed nearly all pre-existing tree seedlings and saplings, stand infilling by post-treatment tree recruitment will be slower in burned units compared to thin-only units (Clyatt et al. 2017), which could extend the persistence of the treatment effects in burned units.

Although we found that the changes in tree growth and tree-ring $\Delta^{13}C$ following thinning improve resistance to drought and bark beetle disturbance, these changes could potentially be overridden under severe, multi-year drought or higher bark beetle pressure. Also, the reduction in mortality over the 23-yr post-treatment period was much lower than the number of trees removed by thinning. Thus, the effects of thinning on drought resistance may not always be strong enough to justify treatments where improving drought resistance is the only objective. However, when thinning is used to restore historical forest structures or reduce the potential for high-severity fire, our analyses support that there is likely to be an additional benefit of improved resistance to drought and related biotic disturbances.

Acknowledgments

We would like to thank Katelynn Bowen, Katie Clyatt, Samantha Farwell, Finn Leary, and Lindsay Grayson for their assistance with the field sampling and tree-ring processing. Duncan Lutes led the formatting, quality control, and organization of the sample plot data. Tony Ward, Carolyn Hester, Bob Yokelson, Vanessa Selimovic, John Maron, and Charlotte Reed provided advice, equipment, and laboratory space for preparing our tree-ring samples. We thank two anonymous reviewers whose helpful feedback improved the manuscript. We acknowledge funding from the Joint Fire Science Program under project JFSP 15-1-07-30.

Literature Cited

Abatzoglou, J. T., S. Z. Dobrowski, S. A. Parks, and K. C. Hegewisch. 2018. TerraClimate, a high-resolution global dataset of monthly climate and climatic water balance from 1958–2015. Scientific Data 5:170191.

Abatzoglou, J. T., and A. P. Williams. 2016. Impact of anthropogenic climate change on wildfire across western US forests. Proceedings of the National Academy of Sciences USA 113:11770–11775.

Adams, H. D., M. Guardiola-Claramonte, G. A. Barron-Gafford, J. C. Villegas, D. D. Breshears, C. B. Zou, P. A. Troch, and T. E. Huxman. 2009. Temperature sensitivity of drought-induced tree mortality portends increased regional die-off under global-change-type drought. Proceedings of the National Academy of Sciences USA 106:7063–7066.

Allen, C. D., D. D. Breshears, and N. G. McDowell. 2015. On underestimation of global vulnerability to tree mortality and forest die-off from hotter drought in the Anthropocene. Ecosphere 6:129.

Allen, C. D., M. Savage, D. A. Falk, K. F. Suckling, T. W. Swetnam, T. Schulke, P. B. Stacey, P. Morgan, M. Hoffman, and J. T. Klingel. 2002. Ecological restoration of southwestern ponderosa pine ecosystems: a broad perspective. Ecological Applications 12:1418–1433.

Anderegg, W. R. L., J. M. Kane, and L. D. L. Anderegg. 2013. Consequences of widespread tree mortality triggered by drought and temperature stress. Nature Climate Change 3:30–36.

Bakaj, F., N. Mietkiewicz, T. T. Veblen, and D. Kulakowski. 2016. The relative importance of tree and stand properties in susceptibility to spruce beetle outbreak in the mid-20th century. Ecosphere 7:e01485.

Barnett, K., S. A. Parks, C. Miller, and H. T. Naughton. 2016. Beyond fuel treatment effectiveness: characterizing interactions between fire and treatments in the US. Forests 7:237.

Biondi, F., and K. Waikul. 2004. DENDROCLIM2002: A C++ program for statistical calibration of climate signals in tree-ring chronologies. Computers & Geosciences 30:303–311.

Bottero, A., A. W. D'Amato, B. J. Palik, J. B. Bradford, S. Fraver, M. A. Battaglia, and L. A. Asherin. 2017. Density-dependent vulnerability of forest ecosystems to drought. Journal of Applied Ecology 54:1605–1614.

Bowen, K. J. 2017. Longevity of ponderosa pine fuel reduction treatments: a legacy of research at Lick Creek Demonstration/Research Forest in western Montana. Thesis. University of Montana, Missoula, Montana, USA.

Bradford, J. B., and D. M. Bell. 2017. A window of opportunity for climate-change adaptation: easing tree mortality by reducing forest basal area. Frontiers in Ecology and the Environment 15:11–17.

Bréda, N., R. Huc, A. Granier, and E. Dreyer. 2006. Temperate forest trees and stands under severe drought: a review of ecophysiological responses, adaptation processes and long-term consequences. Annals of Forest Science 63:625–644.

Breshears, D. D., H. D. Adams, D. Eamus, N. McDowell, D. J. Law, R. E. Will, A. P. Williams, and C. B. Zou. 2013. The critical amplifying role of increasing atmospheric moisture demand on tree mortality and associated regional die-off. Frontiers in Plant Science 4:266.

Castagneri, D., G. Battipaglia, G. von Arx, A. Pacheco, and M. Carrer. 2018. Tree-ring anatomy and carbon isotope ratio show both direct and legacy effects of climate on bimodal xylem formation in *Pinus pinea*. Tree Physiology 38:1098–1109.

Clyatt, K. A., C. R. Keyes, and S. M. Hood. 2017. Long-term effects of fuel treatments on aboveground biomass accumulation in ponderosa pine forests of the northern Rocky Mountains. Forest Ecology and Management 400:587–599.

Condit, R., S. P. Hubbell, and R. B. Foster. 1995. Mortality rates of 205 neotropical tree and shrub species and the impact of a severe drought. Ecological Monographs 65:419–439.

Cook, E. R., and P. J. Krusic. 2014. Program ARSTAN: a tree-ring standardization program based on detrending and autoregressive time series modeling, with interactive graphics. Tree-Ring Laboratory, Lamont Doherty Earth Observatory of Columbia University, Palisades, New York, USA.

Cook, E. R., and K. Peters. 1997. Calculating unbiased tree-ring indices for the study of climatic and environmental change. Holocene 7:361–370.

Cybis Elektronik & Data AB. 2018*a*. CDendro—Cybis dendro dating program. Cybis Elektronik & Data AB, Saltsjöbaden, Sweden.

Cybis Elektronik & Data AB. 2018*b*. Cybis CooRecorder—image coordinate recording program. Cybis Elektronik & Data AB, Saltsjöbaden, Sweden.

D'Amato, A. W., J. B. Bradford, S. Fraver, and B. J. Palik. 2013. Effects of thinning on drought vulnerability and climate response in north temperate forest ecosystems. Ecological Applications 23:1735–1742.

DeLuca, T. H., and K. L. Zouhar. 2000. Effects of selection harvest and prescribed fire on the soil nitrogen status of ponderosa pine forests. Forest Ecology and Management 138:263–271.

Farquhar, G. D., J. R. Ehleringer, and K. T. Hubick. 1989. Carbon isotope discrimination and photosynthesis. Annual Review of Plant Physiology and Plant Molecular Biology 40:503–537.

Fernández-de-Uña, L., N. G. McDowell, I. Cañellas, and G. Gea-Izquierdo. 2016. Disentangling the effect of competition, CO_2 and climate on intrinsic water-use efficiency and tree growth. Journal of Ecology 104:678–690.

Fettig, C. J., K. D. Klepzig, R. F. Billings, A. S. Munson, T. E. Nebeker, J. F. Negrón, and J. T. Nowak. 2007. The effectiveness of vegetation management practices for prevention and control of bark beetle infestations in coniferous forests of the western and southern United States. Forest Ecology and Management 238:24–53.

Friedman, J. H. 1984. A variable span smoother. Stanford University, Lab for Computational Statistics, Stanford, California, USA.

Fulé, P. Z., J. E. Crouse, J. P. Roccaforte, and E. L. Kalies. 2012. Do thinning and/or burning treatments in western USA ponderosa or Jeffrey pine-dominated forests help restore natural fire behavior? Forest Ecology and Management 269:68–81.

Gessler, A., M. Cailleret, J. Joseph, L. Schönbeck, M. Schaub, M. Lehmann, K. Treydte, A. Rigling, G. Timofeeva, and M. Saurer. 2018. Drought induced tree mortality—a tree-ring isotope based conceptual model to assess mechanisms and predispositions. New Phytologist 219:485–490.

Giuggiola, A., J. Ogée, A. Rigling, A. Gessler, H. Bugmann, and K. Treydte. 2016. Improvement of water and light availability after thinning at a xeric site: which matters more? A dual isotope approach. New Phytologist 210:108–121.

Holmes, R. L. 1983. Computer assisted quality control in tree-ring dating and measurement. Tree-Ring Bulletin 44:69–75.

Hood, S. M., S. Baker, and A. Sala. 2016. Fortifying the forest: thinning and burning increase resistance to a bark beetle outbreak and promote forest resilience. Ecological Applications 26:1984–2000.

Hothorn, T., F. Bretz, and P. Westfall. 2008. Simultaneous inference in general parametric models. Biometrical Journal 50:346–363.

Jump, A. S., P. Ruiz-Benito, S. Greenwood, C. D. Allen, T. Kitzberger, R. Fensham, J. Martínez-Vilalta, and F. Lloret. 2017. Structural overshoot of tree growth with climate variability and the global spectrum of drought-induced forest dieback. Global Change Biology 23:3742–3757.

Kalies, E. L., and L. L. Yocom Kent. 2016. Tamm Review: Are fuel treatments effective at achieving ecological and social objectives? A systematic review. Forest Ecology and Management 375:84–95.

Kassambara, A. 2019. rstatix: Pipe-friendly framework for basic statistical tests. R package version 0.3.1. https://cran.r-project.org/web/packages/rstatix/index.html

Khuri, A. I., T. Mathew, and B. K. Sinha. 2011. Statistical tests for mixed linear models. John Wiley & Sons, New York, New York, USA.

Kolb, T. E., K. M. Holmberg, M. R. Wagner, and J. E. Stone. 1998. Regulation of ponderosa pine foliar physiology and insect resistance mechanisms by basal area treatments. Tree Physiology 18:375–381.

Kutner, M. H., C. J. Nachtsheim, J. Neter, and W. Li. 2005. Applied linear statistical models. Fifth edition. McGraw-Hill Irwin, Boston, Massachusetts, USA.

Leavitt, S. W. 2008. Tree-ring isotopic pooling without regard to mass: no difference from averaging δ13C values of each tree. Chemical Geology 252:52–55.

Leavitt, S. W. 2010. Tree-ring C-H–O isotope variability and sampling. Science of the Total Environment 408:5244–5253.

Leavitt, S. W., and S. R. Danzer. 1993. Method for batch processing small wood samples to holocellulose for stable-carbon isotope analysis. Analytical Chemistry 65:87–89.

Lloret, F., E. G. Keeling, and A. Sala. 2011. Components of tree resilience: effects of successive low-growth episodes in old ponderosa pine forests. Oikos 120:1909–1920.

Martin, J., N. Looker, Z. Hoylman, K. Jencso, and J. Hu. 2018. Differential use of winter precipitation by upper and lower elevation Douglas fir in the Northern Rockies. Global Change Biology 24:5607–5621.

Martínez-Vilalta, J., A. Sala, and J. Piñol. 2004. The hydraulic architecture of Pinaceae—a review. Plant Ecology 171:3–13.

McCarroll, D., and N. J. Loader. 2004. Stable isotopes in tree rings. Quaternary Science Reviews 23:771–801.

McDowell, N. G., H. D. Adams, J. D. Bailey, M. Hess, and T. E. Kolb. 2006. Homeostatic maintenance of ponderosa pine gas exchange in response to stand density changes. Ecological Applications 16:1164–1182.

McDowell, N. G., H. D. Adams, J. D. Bailey, and T. E. Kolb. 2007. The role of stand density on growth efficiency, leaf area index, and resin flow in southwestern ponderosa pine forests. Canadian Journal of Forest Research 37:343–355.

Navarro-Cerrillo, R. M., R. Sánchez-Salguero, C. Rodriguez, J. Duque Lazo, J. M. Moreno-Rojas, G. Palacios-Rodriguez, and J. J. Camarero. 2019. Is thinning an alternative when trees could die in response to drought? The case of planted *Pinus nigra* and *P. sylvestris* stands in southern Spain. Forest Ecology and Management 433:313–324.

Negrón, J. F., K. K. Allen, A. Ambourn, B. Cook, and K. Marchand. 2017. Large-scale thinnings, ponderosa pine, and mountain pine beetle in the Black Hills, USA. Forest Science 63:529–536.

Newland, J. A., and T. H. DeLuca. 2000. Influence of fire on native nitrogen-fixing plants and soil nitrogen status in ponderosa pine-Douglas-fir forests in western Montana. Canadian Journal of Forest Research 30:274–282.

Novick, K. A., et al. 2016. The increasing importance of atmospheric demand for ecosystem water and carbon fluxes. Nature Climate Change 6:1023–1027.

R Core Team. 2018. R: a language and environment for statistical computing. R Foundation for Statistical Computing, Vienna, Austria. www.R-project.org

Restaino, C., D. J. N. Young, B. Estes, S. Gross, A. Wuenschel, M. Meyer, and H. Safford. 2019. Forest structure and climate mediate drought-induced tree mortality in forests of the Sierra Nevada, USA. Ecological Applications 29:e01902.

Ruiz-Benito, P., E. R. Lines, L. Gómez-Aparicio, M. A. Zavala, and D. A. Coomes. 2013. Patterns and drivers of tree mortality in Iberian forests: climatic effects are modified by competition. PLoS ONE 8:e56843.

Sala, A., G. D. Peters, L. R. McIntyre, and M. G. Harrington. 2005. Physiological responses of ponderosa pine in western Montana to thinning, prescribed fire and burning season. Tree Physiology 25:339–348.

Sheil, D., D. F. R. P. Burslem, and D. Alder. 1995. The interpretation and misinterpretation of mortality rate measures. Journal of Ecology 83:331–333.

Shore, T. L., and L. Safranyik. 1992. Susceptibility and risk rating systems for the mountain pine beetle in lodgepole pine stands. Information Report-BC-X-336, Pacific Forestry Centre, Pacific and Yukon Region, Victoria, British Columbia, Canada.

Simonin, K., T. E. Kolb, M. Montes-Helu, and G. W. Koch. 2006. Restoration thinning and influence of tree size and leaf area to sapwood area ratio on water relations of *Pinus ponderosa*. Tree Physiology 26:493–503.

Smith, H. Y., and S. F. Arno. 1999. Eighty-eight years of change in a managed ponderosa pine forest. General Technical Report. Rocky Mountain Research Station, Ogden, Utah, USA.

Sohn, J. A., J. R. Brooks, J. Bauhus, M. Kohler, T. E. Kolb, and N. G. McDowell. 2014. Unthinned slow-growing ponderosa pine (*Pinus ponderosa*) trees contain muted isotopic signals in tree rings as compared to thinned trees. Trees 28:1035–1051.

Sohn, J. A., S. Saha, and J. Bauhus. 2016. Potential of forest thinning to mitigate drought stress: a meta-analysis. Forest Ecology and Management 380:261–273.

Szejner, P., W. E. Wright, S. Belmecheri, D. Meko, S. W. Leavitt, J. R. Ehleringer, and R. K. Monson. 2018. Disentangling seasonal and interannual legacies from inferred patterns of forest water and carbon cycling using tree-ring stable isotopes. Global Change Biology 24:5332–5347.

Vaganov, E. A., E.-D. Schulze, M. V. Skomarkova, A. Knohl, W. A. Brand, and C. Roscher. 2009. Intra-annual variability of anatomical structure and δ13C values within tree rings of spruce and pine in alpine, temperate, and boreal Europe. Oecologia 161:729–745.

Vernon, M. J., R. L. Sherriff, P. van Mantgem, and J. M. Kane. 2018. Thinning, tree-growth, and resistance to multi-year drought in a mixed-conifer forest of northern California. Forest Ecology and Management 422:190–198.

Voelker, S. L., A. G. Merschel, F. C. Meinzer, D. E. M. Ulrich, T. A. Spies, and C. J. Still. 2019. Fire deficits have increased drought-sensitivity in dry conifer forests; fire frequency and tree-ring carbon isotope evidence from central Oregon. Global Change Biology 25:1247–1262.

Waring, R. H., and G. B. Pitman. 1985. Modifying lodgepole pine stands to change susceptibility to mountain pine beetle attack. Ecology 66:889–897.

Warren, C. R., J. F. McGrath, and M. A. Adams. 2001. Water availability and carbon isotope discrimination in conifers. Oecologia 127:476–486.

Weed, A. S., M. P. Ayres, and J. A. Hicke. 2013. Consequences of climate change for biotic disturbances in North American forests. Ecological Monographs 83:441–470.

Westerling, A. L. 2016. Increasing western US forest wildfire activity: sensitivity to changes in the timing of spring. Philosophical Transactions of the Royal Society B 371:20150178.

Young, D. J. N., J. T. Stevens, J. M. Earles, J. Moore, A. Ellis, A. L. Jirka, and A. M. Latimer. 2017. Long-term climate and competition explain forest mortality patterns under extreme drought. Ecology Letters 20:78–86.

Zang, C., and F. Biondi. 2013. Dendroclimatic calibration in R: the bootRes package for response and correlation function analysis. Dendrochronologia 31:68–74.

Zhang, J., M. W. Ritchie, D. A. Maguire, and W. W. Oliver. 2013. Thinning ponderosa pine (*Pinus ponderosa*) stands reduces mortality while maintaining stand productivity. Canadian Journal of Forest Research 43:311–320.

Supporting Information

Additional supporting information may be found online at: http://onlinelibrary.wiley.com/doi/10.1002/eap.2188/full

Data Availability

The two primary data sets used in this study are available at the U.S. Forest Service Research Data Archive. The sample plot data used to evaluate changes in tree density, basal area, and tree mortality following the treatments are available at https://doi.org/10.2737/RDS-2020-0008. The tree-ring growth and stable-carbon isotope data are available at https://doi.org/10.2737/RDS-2020-0027.